

## Article

## MPP1 as a Factor Regulating Phase Separation in Giant Plasma Membrane-Derived Vesicles

Joanna Podkalicka,<sup>1,4</sup> Agnieszka Biernatowska,<sup>1</sup> Michał Majkowski,<sup>1</sup> Michał Grzybek,<sup>2,3</sup> and Aleksander F. Sikorski<sup>1,\*</sup>

<sup>1</sup>Laboratory of Cytochemistry, Faculty of Biotechnology, University of Wrocław, Wrocław, Poland; <sup>2</sup>Paul Langerhans Institute Dresden of the Helmholtz Centre Munich at the University Clinic Carl Gustav Carus, TU Dresden, Dresden, Germany; <sup>3</sup>German Center for Diabetes Research (DZD e.v.), Neuherberg, Germany; and <sup>4</sup>Max Planck Institute of Molecular Cell Biology and Genetics, Dresden, Germany

**ABSTRACT** The existence of membrane-rafts helps to conceptually understand the spatiotemporal organization of membrane-associated events (signaling, fusion, fission, etc.). However, as rafts themselves are nanoscopic, dynamic, and transient assemblies, they cannot be directly observed in a metabolizing cell by traditional microscopy. The observation of phase separation in giant plasma membrane-derived vesicles from live cells is a powerful tool for studying lateral heterogeneity in eukaryotic cell membranes, specifically in the context of membrane rafts. Microscopic phase separation is detectable by fluorescent labeling, followed by cooling of the membranes below their miscibility phase transition temperature. It remains unclear, however, if this lipid-driven process is tuneable in any way by interactions with proteins. Here, we demonstrate that MPP1, a member of the MAGUK family, can modulate membrane properties such as the fluidity and phase separation capability of giant plasma membrane-derived vesicles. Our data suggest that physicochemical domain properties of the membrane can be modulated, without major changes in lipid composition, through proteins such as MPP1.

## INTRODUCTION

Rafts are functional assemblies of lipids and proteins present in the membranes of living cells, wherein bioactivity is dependent on synergistic interactions between their components (1). Their metastable nature and nanoscopic size can only be captured with sophisticated, high-resolution techniques (2) because they cannot be directly observed by using conventional microscopy. The observation of large-scale phase separation in cell membrane-derived spheres and vesicles (giant plasma membrane-derived vesicles, GPMVs) is the most convincing evidence of the underlying lateral heterogeneity of the membrane (3–6). Observation of such microscopic phases is possible due to the coalescence of the metastable, nanoscopic, resting state membrane rafts present in the plasma membrane of the living cell (7), which fuse into a condensed liquid-ordered ( $l_o$ ) phase under certain physicochemical conditions. This process is most likely the result of specific lateral associations of lipids, which follow the phase-separation principles observed in model membranes and which involve a mixture of chemical interactions, such as hydrogen bonds, van der Waals attractions, hydrophobic/hydrophilic interactions, and electrostatic forces. The biochemical composition of GPMVs represents, to a

significant degree, their original membranes and therefore, they have become a valuable tool for membrane research (5,6).

The analysis of the phase-separation properties and partitioning of various membrane components has prompted speculation concerning the composition and the physical properties of the underlying raft assemblies (5). Although membrane components separate only into two phases, their individual properties can vary, and each phase can span a number of different states, dependent on the composition of the membranes of origin, or the GPMV isolation method used (5,8). The temperature at which  $l_o$  and liquid-disordered ( $l_d$ ) phases separate varies between cell types, which is the consequence of cell-specific membrane composition. Interestingly, the phase-separation temperature of GPMVs isolated even from one cell type can vary, because it is sensitive to receptor ligand-binding or changes of membrane lipid composition (5,6,9,10). It has also been demonstrated that membrane partitioning of amphiphiles can greatly affect domain formation (11). It remains however unclear, what other means apart from changes in lipid composition are used by the cells to tune raft properties.

The ubiquitously expressed MAGUK family of proteins (12) has been proposed to be important for formation and function of synapses (13–15), for the formation and maintenance of several types of cell junctions (14,16–18), and mediating antibody recognition in hematopoietic cells (19). All MAGUKs share several domains including PDZ,

Submitted August 6, 2014, and accepted for publication March 10, 2015.

\*Correspondence: [afsbc@ibmb.uni.wroc.pl](mailto:afsbc@ibmb.uni.wroc.pl)

This is an open access article under the CC BY-NC-ND license (<http://creativecommons.org/licenses/by-nc-nd/4.0/>).

Editor: Tobias Baumgart.

© 2015 The Authors  
0006-3495/15/05/2201/11 \$2.00



SH3, and a guanylate-kinase homology domain. In addition, some MAGUKs contain an N-terminus homologous to CaM kinase with a calmodulin-binding site (20,21). The simplest member of this family is MPP1 (membrane palmitoylated protein 1, p55), which was originally found in erythrocytes (22), where it acts as a scaffold protein that links the membrane skeleton to the plasma membrane by forming a tripartite complex with protein 4.1 and glyco-phorin C (22). MPP1 has also been suggested to regulate neutrophil polarity and to function as a positive upstream effector of Akt phosphorylation (23). In addition, we have previously shown that lack of MPP1 palmitoylation in human erythrocytes clinically manifests as severe hemolytic anemia, arising as a consequence of alterations in the lateral organization of the plasma membrane (24,25). Moreover, knockdown of *MPP1* in erythrocyte precursors, human erythroleukemia (HEL) cells, caused significant reduction of the isolated detergent-resistant membrane (DRM) fraction and impaired relative order within the plasma membrane, leading to reduced phosphorylation of Erk1/2 kinase upon insulin-receptor/c-kit activation (25). Altogether, these results have led us to speculate about the novel role of MPP1 in regulating plasma membrane lateral heterogeneity.

Here, we further explore the role of MPP1 in membrane organization and demonstrate that the presence of this protein can alter the physicochemical properties of the plasma membrane by increasing the packing of lipids. Using GPMVs, essentially a cytoskeleton-free plasma membrane model, generated from HEL cells with silenced expression of MPP1, we demonstrate that reduction of MPP1 content leads to changes in membrane fluidity and the phase separation properties of plasma membrane vesicles. Decrease in the miscibility transition temperature ( $T_{\text{misc}}$ ), as well as plasma membrane order alterations, observed by several different fluorescence imaging techniques, imply that MPP1 takes part in coalescence of naturally occurring nano-assemblies in the native membrane. To our knowledge, our results indicate a novel and remarkable role of so far, poorly characterized MAGUK family protein member, MPP1, as a scaffold molecule responsible for plasma membrane lateral structure organization of erythrocyte precursors. This membrane-organization property may also be a feature of other MAGUK family proteins and other cell membranes.

## MATERIALS AND METHODS

### Cell culture and gene silencing

HEL cells were grown in RPMI 1640 medium supplemented with 10% fetal calf serum, 2 mM glutamine, 100 units/mL penicillin, and 100  $\mu\text{g}/\text{mL}$  streptomycin at 37°C in a humidified atmosphere of 5%  $\text{CO}_2$ . MPP1-knockdown (KnD) and scrambled control cells were grown in a similar medium, supplemented additionally with 2  $\mu\text{g}/\text{mL}$  puromycin. *MPP1* gene silencing was performed as described (25).

### Plasmids and antibodies

The MPP1-green fluorescent protein (GFP) construct was obtained by cloning the *MPP1* gene sequence into the pEGFP-C1 vector (Invitrogen, Waltham, MA) using BamHI and XhoI restriction sites. To obtain a MPP1 rescue mutant (MPP1-R), the MPP1 sequence was cloned into the p3XFLAG-CMV-10 vector (Sigma, St. Louis, MO) using HindIII and BamHI restriction sites and subsequently modified by introducing four silent mutations in the region recognized by the shRNA sequence using site-directed mutagenesis (Stratagene, Waltham, MA) (primer sequence: 5' GGAGATGACGAGGA ACATTAGCGCCAATGAGTTCCTTG 3'). Abp140-17aaRuby-nos1-3' UTR (lifeAct-Ruby) construct was a gift from M. C. Lecomte U665 INSERM Paris. Transient transfections of HEL cells were performed by CLB (Lonza, Basel, Switzerland) electroporation. Mouse monoclonal anti-MPP1 antibodies were purchased from Abnova (Taipei, Taiwan), anti-actin and anti-GFP antibodies (SantaCruz Biotechnology, Dallas, TX), anti-Flag (Sigma), anti-Flotillin-1 (Abcam, Cambridge, UK), anti-Furin Convertase (Thermo Fisher Scientific, Waltham, MA), anti-Calnexin (Stressgen, San Diego, CA).

### GPMV generation, membrane labeling, and MPP1 localization

GPMVs were isolated, using vesiculation buffer (10 mM HEPES, 2 mM  $\text{CaCl}_2$ , 2 mM NEM, pH 7.25) as previously described (26), additionally supplemented with 2  $\mu\text{M}$   $\text{NaVO}_4$  and 1  $\mu\text{g}/\text{mL}$  U73122 (PI-PLC inhibitor, Tocris Bioscience, Bristol, UK). GPMVs were stained with C-laurdan (2  $\mu\text{M}$ ) (15 min/RT) or Fast-DiO (5  $\mu\text{g}/\text{mL}$ ) (10 min/RT) (Invitrogen). A chamber was created by making a square of silicon sealant (Baysilone Paste, GE Bayer Silicone, Leverkusen, Germany) on a bovine serum albumin-coated cover slip, into the center of which 30  $\mu\text{l}$  of labeled GPMV suspension was deposited, followed by sealing of the chamber with another cover slip, as described (27). For imaging, a Zeiss inverted wide-field charge-coupled device microscope with appropriate filter sets and a 40 $\times$  air-objective was used. General polarization (GP) measurements were acquired by two-photon microscopy of C-Laurdan in phase-separated GPMVs at 4°C using the Bio-Rad (Hercules, CA) two-photon setup with a Mira 2000 two-photon laser and a 543-nm laser line using a 60 $\times$  WI objective (NA 1.2), as described (7). For order analysis, collected GPMVs were stained with 7.5  $\mu\text{M}$  di-4ANEPHPH (di-4, Invitrogen) probe (10 min/RT) and introduced into a sealed chamber, this time coated with poly-L-lysine. di-4 fluorescence lifetime measurements were acquired by time-correlated single-photon counting (TCSPC) using a LSM 510 META microscope (Carl Zeiss, Jena, Germany) equipped with fluorescence lifetime imaging microscopy (FLIM) and fluorescence correlation spectroscopy dedicated optics from PicoQuant (Berlin, Germany). Samples were excited at 470 nm and imaged with a 40 $\times$  WI objective (NA 1.2) using an LP 500 filter set. Acquisition time was adjusted to collect at least 1000 photons per pixel. Each pixel in the image was pseudocolored according to the average fluorescent lifetime. For  $T_{\text{misc}}$ , phase transition was assessed for  $\geq 30$  vesicles/temperature and the fraction of separated vesicles plotted against temperature was fitted with sigmoidal curve. The point of the curve representing 50% of phase-separated vesicles was defined as  $T_{\text{misc}}$ . For confocal microscopy analysis of MPP1 localization to GPMVs, a Zeiss LSM 510 META microscope with LP 500 filter and a 40 $\times$  WI objective was used.

### GPMV isolation and protein profile analysis

GPMVs were separated from cells using density-gradient ultracentrifugation. GPMVs were stratified in a 15% Optiprep solution (Sigma) and ultracentrifuged (40,000 rpm/30 min/4°C). The resultant lipid fraction containing GPMVs was collected. The sample was diluted twofold in 150 mM NaCl, 25 mM HEPES pH 7.25 and ultracentrifuged (45,000 rpm/30 min/4°C). Pelleted membranes were dissolved in 50  $\mu\text{l}$  of

GPMV vesiculation buffer. Protein concentration was determined by BCA. SDS-PAGE (NuPAGE, Invitrogen) and Western blot were used to analyze the proteins.

### Thin layer chromatography and lipids fluidity analysis

GPMV-enriched fractions obtained after gradient separation were extracted using a two-step extraction protocol (chloroform/methanol 10:1, followed by chloroform/methanol 2:1) (27). The lipid-containing organic phases from both steps were pooled and dried under a nitrogen stream. For thin layer chromatography (TLC) analysis, lipids were dissolved in 30  $\mu$ l of chloroform/methanol (2:1) and applied to a TLC plate. A 9:7:2 mixture of chloroform/methanol/ammonia (25% solution) was used as a running phase for TLC analysis. The lipids were visualized by spraying the plate with 20%  $H_2SO_4$  solution and heating (200°C, 3–5 min). For fluidity analysis, dried lipids were rehydrated in 150 mM NaCl, 25 mM HEPES pH 7.25. The resulting liposomes were subsequently subjected to 10 freezing/thawing cycles (liquid nitrogen/37°C). Finally, vesicles were stained (15 min) with 2  $\mu$ M C-laurdan. Fluorescence emission spectra were recorded (Ex. 385 nm, Em. 400–550 nm) and analyzed as described (7).

### Image analysis

GP image analysis was performed using MATLAB R2006B (The MathWorks, Natick, MA) as described (7). Briefly, all images were normalized and background corrected. GP images were masked and displayed in twofold binned heat maps according to the following Eq. 1:  $GP = I_{CH1} - G \cdot I_{CH2} / I_{CH1} + G \cdot I_{CH2}$ , where  $G$  served to calibrate channels (28). Pixels below 20% of the maximum signal were masked black and not considered for further analysis. Confocal images were obtained using ZEN 2009 Light Edition software. All images were contrast-enhanced using ImageJ software. Di-4 lifetime distribution was analyzed by applying a mask over a region of interest.

## RESULTS AND DISCUSSION

### MPP1 modulates membrane order

We have suggested previously that MPP1 regulates lateral organization of erythrocyte/erythroid cell membrane and influences signal transduction pathways, showing its physiological importance (24,25). Here, we decided to study the role of MPP1 on membrane organization in more detail, considering its influence on plasma membrane physicochemical properties in model membranes, such as GPMVs. First, we characterized relative lipid packing of GPMVs obtained from cells transduced with lentiviruses containing either a short antisense, hairpin-RNA targeting MPP1 (KnD), or a scrambled control shRNA (SC). MPP1-targeted cells showed a reproducible decrease of MPP1 level to ~20% of control (Fig. 1 A). This reduction had no influence on cell growth. GPMVs obtained from these cells were doped with di-4 probe, which is commonly used as a reporter of lipid-packing, because it senses water incorporation within the bilayer. Fluorescence lifetime shifts toward longer values when lipids are more condensed (29,30). The performed measurements are sensitive even to subtle changes in membrane order. In our hands, in giant unilamel-

lar vesicles composed only from dioleoyl-phosphatidylcholine (DOPC) or palmitoyl-oleoyl-phosphatidylcholine (POPC), di-4 fluorescence lifetime values vary between 2 and 2.3 ns, respectively, whereas for vesicles composed of DOPC/sphingomyelin (SM)/cholesterol (Chol) (1:1:2) di-4 lifetime shifts to around 4 ns (31). Di-4 present in GPMVs obtained from MPP1-KnD cells showed significantly shorter fluorescence lifetime values (~3.18 ns) than in the control GPMVs (~3.82 ns for control and ~3.69 ns for SC) (Fig. 1, B–D). The difference in di-4 lifetime values suggests that membranes in GPMVs isolated from MPP1-KnD cells are more loosely packed than those from the control cells. Such a result confirms our previous observations performed on live cells, where we also determined that, upon *MPP1* silencing, the order of the plasma membrane was reduced (25). It should be noted, however, that the observed difference in di-4 lifetime values between the control and MPP1-KnD samples measured for GPMVs were more pronounced than was observed previously for live cells from which the GPMVs were prepared ( $\Delta$ GPMV ~0.5 ns vs.  $\Delta$ live cells ~0.3 ns). This might imply that either the metabolizing cells are able to buffer the changes caused by MPP1 depletion, or, that the previous measurements were partially biased by signal from internal membranes. In any case, GPMVs seem to be superior, as they allow the analysis of only the changes that relate to the plasma membranes.

Temperature-dependent phase separation of GPMVs has been used previously to analyze and characterize the partitioning of various proteins (6). Although using di-4 and FLIM allows us to observe subtle changes of membrane order, this type of measurement unfortunately does not allow the precise measurement of the order of the respective phases in phase-separated vesicles, because it takes a relatively long time to measure the lifetime values (usually 1–2 min), during which the dynamic phases move across the vesicles. Therefore, the information that one gets is an average value of both phases. Therefore, to obtain more insight into the manner by which MPP1 influences one or the other phase in phase-separated vesicles, we performed measurements using another reporter of membrane order, C-laurdan. This has been previously used by others to analyze membrane order in phase-separated vesicles at 4°C. The emission peak of the dye shows a characteristic shift toward shorter wavelengths (maximal emission at 440 nm), the same principle as for di-4 probe, when lipids are relatively more ordered, compared to less ordered membranes (with emission maximum at 490 nm). To normalize relative membrane lipid packing, a GP value can be calculated from the described emission shift, as shown by Kaiser and co-workers (7). Once again we noticed that reduction of MPP1 content resulted in physicochemical changes of the plasma membrane, reflected as a significantly lower mean GP value obtained for GPMVs isolated from MPP1-KnD cells in comparison to those obtained from controls

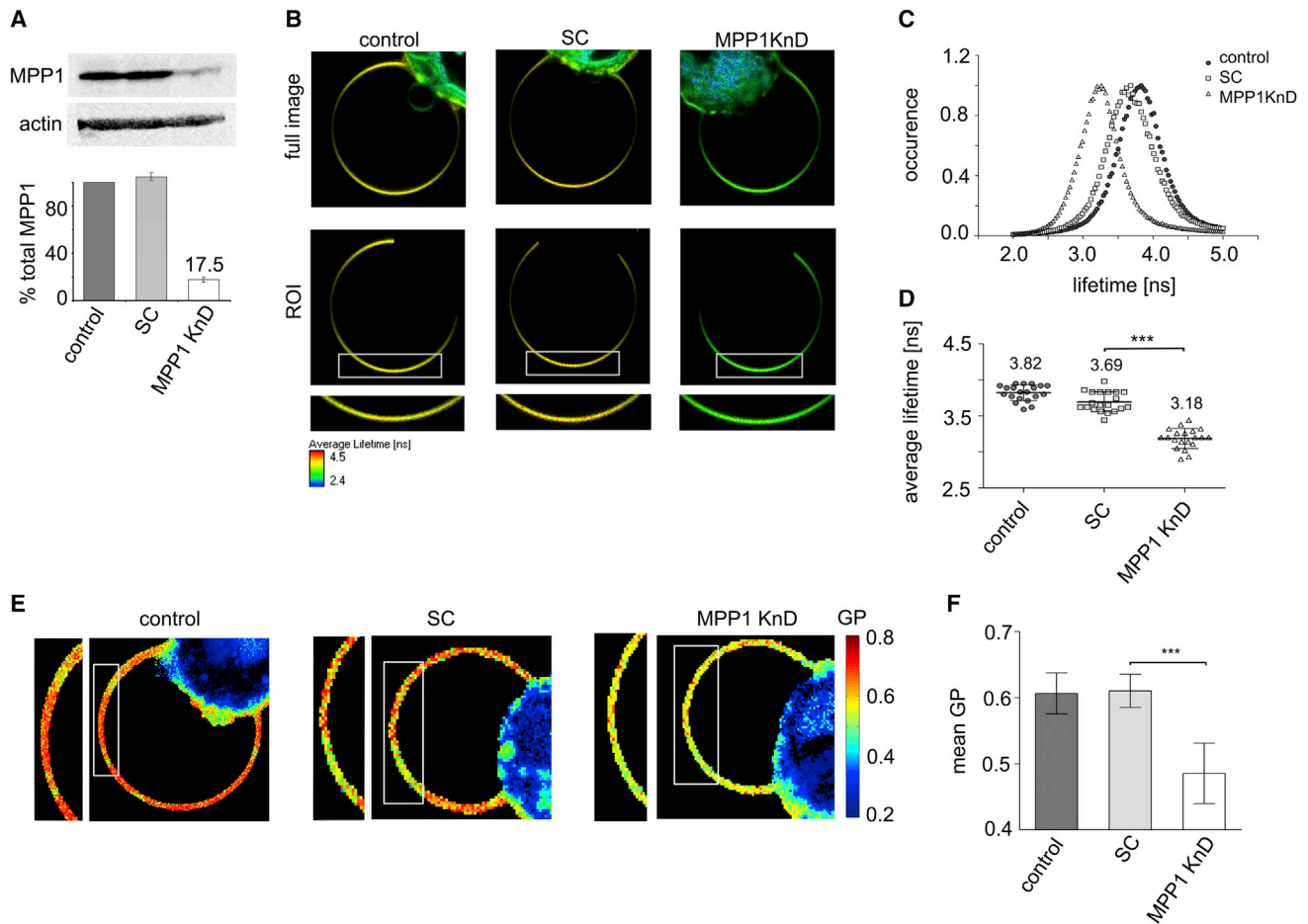


**FIGURE 1** MPP1 reduction increases GPMV membrane fluidity. (A) Western blot analysis and quantification of MPP1 expression level in MPP1-KnD cells (data is an average from three independent experiments). (B) Representative FLIM images of di-4 stained GPMVs isolated from MPP1-KnD and control cells (the longer the fluorescence lifetime values, the more ordered the membrane; all images taken at 23°C). (C) Fluorescence lifetime histograms. Points represent an average of >30 vesicles per cell type. (D) Quantitative analysis of di-4 fluorescence lifetime distribution of GPMVs obtained from MPP1-KnD and control cells shows significant reduction of fluorescence lifetime values in the absence of MPP1 (average from 15 vesicles per cell type, representing three independent experiments). (E) Exemplary, masked GP images of C-laurdan stained GPMVs (higher GP value correlate with a more ordered membrane; all images were taken at 4°C). (F) Average GP is lower for vesicles obtained from MPP1-KnD cells compared to control. Each point is representative of >40 vesicles per cell type. ROI, region of interest. Differences were considered statistically significant at \*\*\* $p < 0.001$ . To see this figure in color, go online.

(Fig. 1, E and F). This result, although obtained at a much lower temperature, is in line with the previously described lifetime measurements and indicated that the presence of MPP1 at the plasma membrane can increase relative membrane packing independently of temperature conditions of the experiment.

It was previously shown that the method of GPMV isolation could substantially affect membrane behavior and phase-separation properties. Application of compounds such as paraformaldehyde/dithiothreitol, leading to the cross-linking of proteins, resulted in stabilization of the observed phases, as reflected by the relatively high  $\Delta$ GP values (6,32). As we used NEM (*N*-ethylmaleimide), a non-cross-linking and nonreducing compound, for GPMV generation, the observed differences in GP between GPMVs derived from MPP1-KnD cells and control cells are relatively small ( $\sim 0.1$ ) (Fig. 1 F). The measured order param-

eters of the  $I_o$  and  $I_d$  phases in phase-separated vesicles suggest that both phases observed for MPP1-KnD GPMVs are less ordered than their control equivalents. Noteworthy,  $\Delta$ GP (defined as the difference between the GP obtained for the ordered and disordered phase) is constant for all three types of GPMVs ( $\Delta$ GP $\sim 0.05$ ) (Fig. S1 in the Supporting Material). This observation is particularly interesting because it suggests that the lack of stabilization of protein-lipid nanoassemblies present in the native membrane can lead to increased mixing of components.

Significantly lower GP values, as well as shorter di-4 fluorescence lifetime values, were detected for MPP1-KnD-derived vesicles, reflecting changes in the physicochemical properties of the plasma membrane, suggesting impaired raft formation as a result of *MPP1* gene silencing. The mechanism proposed here is in accordance with the model of plasma membrane lateral organization, which highlights

the dominant role of proteins in capturing and stabilizing highly dynamic and unstable ordered domains. This forms the basis of the concept of plasma membrane compartmentalization and the variety of membrane microdomain sizes observed (33).

To confirm that MPP1 localizes to the plasma membrane of HEL cells and that it is associated with the membrane after GPMV isolation, we transiently transfected these cells with MPP1-GFP vector and subsequently isolated GPMVs from them. The MPP1-GFP expression level in whole cell lysate was around 5 times higher than endogenous MPP1 (Fig. 2, A and B). After induction of membrane blebbing, the GFP signal was predominantly associated with internal cell structures. However, a fraction of the GFP signal was also bound to the membrane of GPMVs (Fig. 2 C), indicating that the previously observed changes in membrane organization may be regulated by the membrane-bound fraction of MPP1. This seems to be a minor fraction, which is not surprising, as our previous results indicated that even though only a small portion of MPP1 (most probably palmitoylated MPP1) stays bound to the erythrocyte DRM fraction, it is still able to trigger changes in membrane order leading to hemolytic anemia (24). In contrast, the nonpalmitoylated MPP1 remains attached to the cortical cytoskeleton (25), which is absent in GPMVs. Moreover, overexpression

of MPP1 in control cells did not trigger further increase in plasma membrane order, manifested as no changes in di-4 fluorescence lifetime values (Fig. S2), suggesting that the MPP1/membrane interactions are saturated.

### MPP1 triggers fluidity changes within the membrane without major alterations in lipid composition

The observed changes in membrane order caused by MPP1 knockdown suggest an important role for this protein in controlling membrane fluidity. However, as mentioned previously, the results from the genetic approach used here could also be a consequence of changes in plasma membrane lipid composition arising from a separate mechanism of membrane lipid control, and not just simply a consequence of reduction of MPP1 protein in the cells. We therefore decided to isolate GPMVs and perform lipid composition analysis of these vesicles. As the studied cells grow in suspension, the isolation of GPMVs is not as straightforward as for adherent cells. We used flotation in a density gradient to obtain GPMV-enriched fractions from these cells. Biochemical analysis of the floating vesicles indicated that these samples consisted predominantly of plasma membranes, as all of the endomembrane markers that were tested,

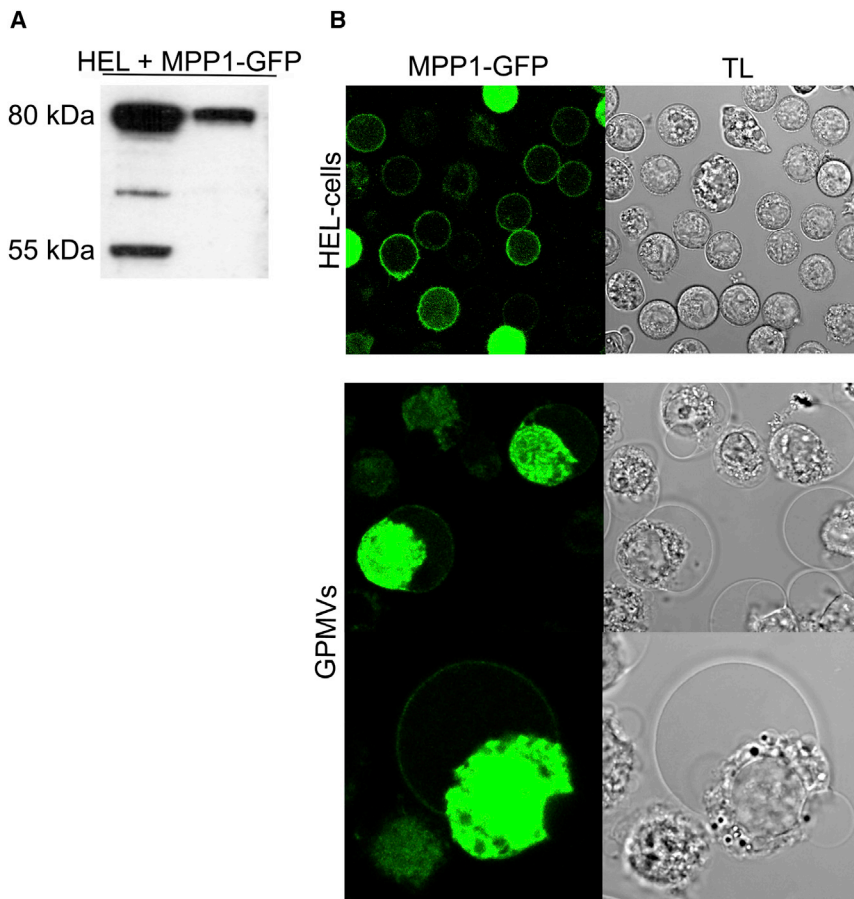
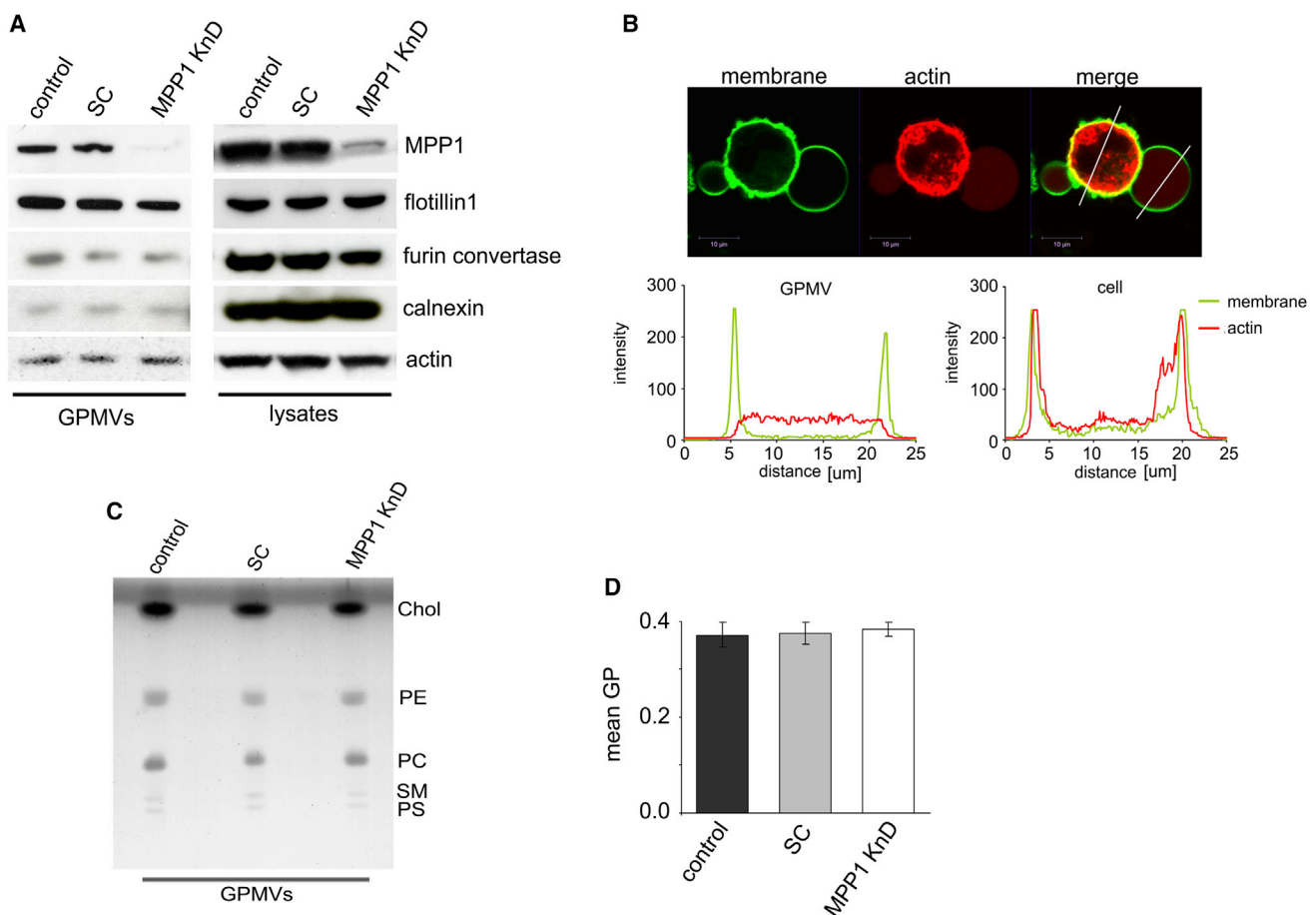


FIGURE 2 MPP1 interacts with the membrane and localizes to GPMVs. (A) Western blot analysis of MPP1-GFP and endogenous MPP1 expression levels in HEL cells. (B) Representative images of MPP1-GFP localization in HEL cells. To see this figure in color, go online.

i.e., calnexin (endoplasmic reticulum) and furin convertase (Golgi), were significantly depleted in this preparation (Fig. 3 A). However, some of these markers were still present in the vesicle-enriched fraction, due to not ideal GPMV/cell separation (Fig. S3). To prove that no cortical actin was present within the GPMVs, we transiently expressed life-act-Ruby in HEL cells, which encodes a peptide with high affinity to cortical actin fused with red fluorescent protein. After GPMV induction, vesicles were additionally stained with Fast-DiO to visualize the membrane. Analysis of the resulting GPMVs confirmed that cortical actin was not present in the GPMV membranes (Fig. 3 B). After extracting the samples with organic solvents, we performed TLC. No observable differences between the compositions of the major lipid-classes were noticed (Fig. 3 C), suggesting that the lipid composition of the plasma membrane seems rather similar between the MPP1-KnD and controls. However, because TLC analysis does not discriminate between chain length

or saturation levels of fatty acids within the class, and is not sensitive enough to detect low-abundant lipid species, we decided to use another approach to further analyze the lipid components. The lipids extracted from the floating fraction of GPMVs were rehydrated to form lipid vesicles, which were subsequently used for measurements of membrane order with C-laurdan. Spectrofluorimetric analysis revealed that the samples did not differ in membrane order parameter (GP) (Fig. 3 D), thereby, further strengthening the argument that lipid composition is similar in MPP1-KnD and control cells, and implying that binding of MPP1 to the membrane affects its fluidity. As one cannot exclude discrete changes in lipid composition between the analyzed samples stronger conclusions could be drawn if more detailed lipidomics data were available.

Finally, to validate whether the observed changes in membrane order can be restored, and are not a result of the off-target effect of *MPP1*-gene silencing, we performed



**FIGURE 3** Alteration in membrane order is not a consequence of major changes in lipid composition (A) Western blot analysis of GPMVs (*left*) and whole cell lysates (*right*). Gradient-separated GPMV fraction contains markedly decreased endoplasmic reticulum (calnexin), Golgi (furin convertase), and cytoskeletal (actin) markers. No significant changes were observed in the abundance of cellular compartment protein markers between cell types. (B) Representative image of cortical-actin localization in GPMV derived from HEL cell. Red, cortical actin visualized by lifeAct-Ruby; green, membranes stained with Fast-DiO. (C) TLC of lipids extracted from GPMVs. No changes observed in the major lipid classes for GPMVs isolated from KnD versus control cells. Chol, cholesterol; PE, phosphatidylethanolamine; PC, phosphatidylcholine; SM, sphingomyelin; PS, phosphatidylserine. (D) Spectrofluorimetric analysis of C-laurdan stained vesicles prepared from GPMVs-extracted lipids obtained from analyzed cell lines. No detectable changes in membrane fluidity were observed between the samples (average from three independent experiments). To see this figure in color, go online.

a rescue experiment in MPP1-KnD cells by introducing a number of silent mutations into the sequence region recognized by an shRNA targeting MPP1, cloning it into a flag vector and subsequently transfecting it into MPP1-KnD cells. MPP1 expression was restored approximately to the level of endogenous MPP1 in control cells (Fig. 4 A). Interestingly, the introduced vector seemed to restore endogenous MPP1 as well. It was shown that shRNAs recognizing a partially complementary target sequence (in our case the MPP1-R sequence) also lead to recruitment of the RISC complex (RNA-induced silencing complex). In this case, instead of mRNA degradation, RISC is arrested on mRNA and inhibition of translation is observed (reviewed in (34)). Saturation of RISC is demonstrable in cultured cells (35). Furthermore, once RISC is arrested, it could result in recovery of endogenous protein expression, as there is no complex available for target mRNA degradation. GPMVs isolated from the MPP1-R (rescue) and stained with di-4 probe, showed recovery of membrane order, as the di-4 lifetime values were almost identical to those obtained for control GPMVs (MPP1-KnD –  $3.27 \pm 0.1$  ns, SC –  $3.67 \pm 0.1$  ns, MPP1-R –  $3.57 \pm 0.1$  ns) (Fig. 4, B and C), suggesting that the observed change of membrane order is predominantly modulated by the presence of MPP1.

### Reduced level of MPP1 significantly decreases the miscibility transition temperature in GPMVs

The observed coexistence of  $l_o/l_d$  phase separation in GPMVs, resulting from temperature-dependent coalescence

of membrane domains present under physiological conditions in cellular membranes, provides an excellent tool for the investigation of raft composition as well as their physical properties (3,4,9,11,36–39). GPMVs isolated either from MPP1-KnD or control cells separated into two distinct microscopically observable phases, which were visualized by doping the membranes with Fast-DiO probe, which displays nonuniform phase partitioning to the  $l_d$  phase (6,11,26). Strikingly, we noticed that the presence of MPP1 stabilized the coexistence of the two liquid phases, and that this could be observed at higher temperatures in the case of GPMVs isolated from control cells than those derived from MPP1-KnD cells (Fig. 5 A). Although the  $T_{misc}$  (defined as the temperature at which 50% of vesicles remain phase separated) for vesicles derived from control and SC cells oscillated around  $17^\circ\text{C}$  (mean  $T_{misc} = 17.1 \pm 0.5$  for control,  $T_{misc} = 16.6 \pm 0.2$  for scrambled), it was  $\sim 2^\circ\text{C}$  lower ( $T_{misc} = 15.1 \pm 0.3$ ;) for vesicles derived from MPP1-KnD cells (Fig. 5, B and C), pointing to an essential engagement of MPP1 in the stabilization of preexisting nanoassemblies. Interestingly, the miscibility transition temperatures obtained for NEM-induced GPMVs are relatively high in comparison to values presented by others (6,11). Nevertheless, it has to be stressed that previous studies were done exclusively on adherent cells, whereas HEL cells grow in suspension, which can influence membrane behavior. Moreover, as HEL cells are erythroid precursors their plasma membrane most probably mimics closely the membranes of erythrocytes, which are known to contain quite high levels of cholesterol (up to

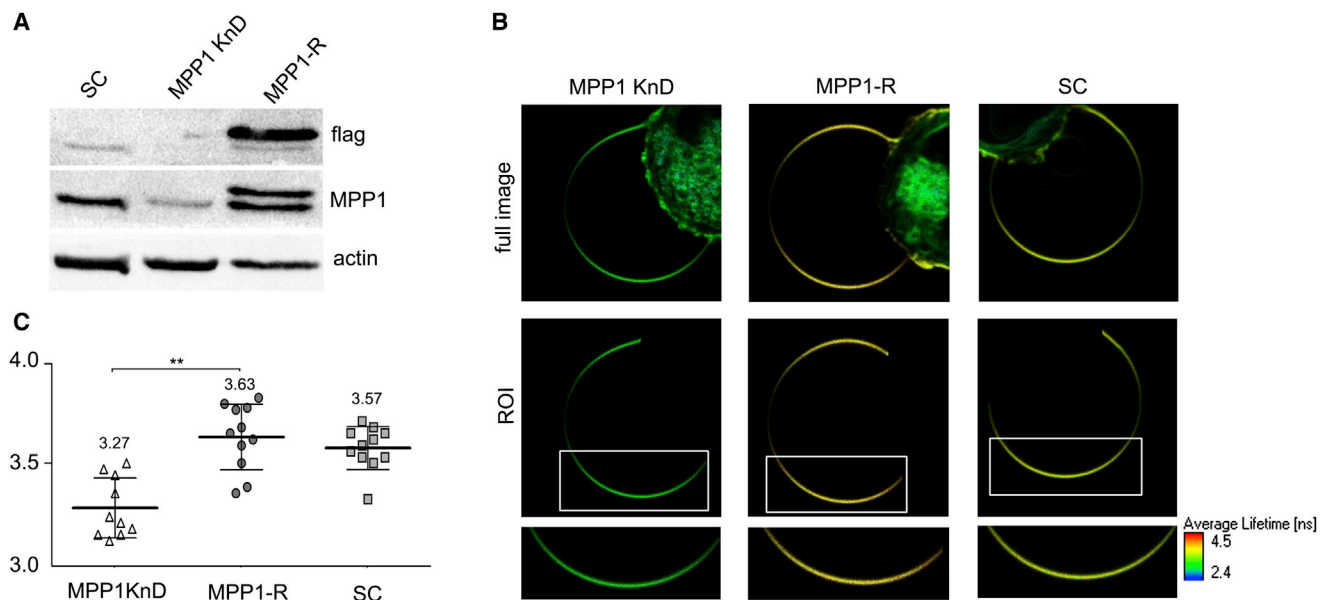


FIGURE 4 MPP1 rescue increases the lifetime value of di-4 in KnD cells. (A) Western blot analysis of *MPP1* expression level after its rescue in MPP1-KnD cells. *MPP1* expression was restored to the level of control. (B) Representative FLIM images of di-4 stained GPMVs isolated from MPP1-KnD rescued cells. (C) Quantitative analysis of di-4 fluorescence lifetime distribution in GPMVs obtained from MPP1-KnD, MPP1-R, and SC cells shows significant increase of fluorescence lifetime values after MPP1 recovery (average from 10 vesicles per cell type, representing three independent experiments). ROI – region of interest. Differences were considered statistically significant at  $**p < 0.01$ . To see this figure in color, go online.

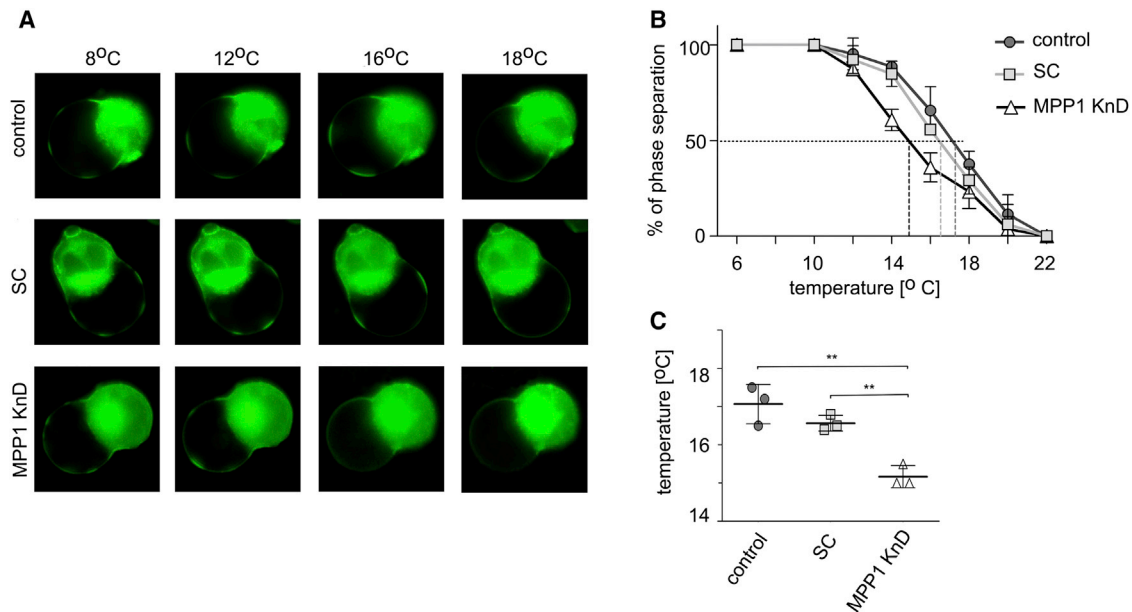


FIGURE 5 *MPP1* knockdown causes a shift in the temperature of phase separation of GPMVs. (A) Representative images and (B) quantification of phase separation in GPMVs isolated from different cell types, measured at various temperatures. Phase separation in vesicles obtained from knockdown cells is observable approximately up to 15°C, whereas control vesicles remain phase separated up to 17°C. Points are an average of  $\pm 10$  vesicles per cell type, representative of three independent experiments. (C) Average temperature at which phase separation occurs ( $T_{misc}$ , defined as the temperature at which 50% of vesicles remain phase separated) of GPMVs isolated from different cell types.  $T_{misc}$  of vesicles isolated from MPP1-KnD cells is  $\sim 2^\circ\text{C}$  lower compared to control. Differences were considered statistically significant at  $**p < 0.01$ . To see this figure in color, go online.

40 mol %). As was shown previously, the cholesterol/phospholipid ratio has a strong influence on membrane phase behavior (9). The molar ratio of phospholipids/cholesterol in the plasma membrane of other cell types is usually  $\sim 1$  (40). It was also demonstrated that some compounds, such as bile acids, can stabilize phase separation in GPMVs without affecting protein behavior between coexisting domains, through their partitioning to and further disordering the  $l_d$  domain, thus promoting phase separation by increasing domain immiscibility (11). Although the MPP1-dependent change in  $T_{misc}$  of  $2^\circ\text{C}$  could be considered as quite a minor effect, it needs to be pointed out that even externally added proteins which are known to trigger strong domain-clustering and stabilization, such as cholera toxin subunit B or Annexin V, shift the miscibility transition temperature by around  $4^\circ\text{C}$  (10). In this context, with endogenous, membrane bound MPP1 present at relatively low amounts at the membrane, a  $2^\circ\text{C}$  shift in  $T_{misc}$  represents a noticeable change, pointing to a role of MPP1 in membrane domain stabilization.

As has been previously shown by others, a number of factors can influence phase separation properties of GPMVs. However, so far, all these reported changes between the  $T_{misc}$  of the  $l_o$  and  $l_d$  phases were caused either by changes in the lipid composition of the isolated GPMVs or by exogenous addition of cross-linking or clustering factors, which are not regulated by the cells (3,6,11). To our knowledge, we show for the first time that stabilization of membrane domain immiscibility, observed as a shift in  $T_{misc}$  of  $l_o$

and  $l_d$  phases, can be specifically modulated by MPP1 protein. The method applied in this study for the isolation of GPMVs is based on noncross-linking and nonreducing chemical conditions using NEM and the resulting vesicles mirror closely the composition of native plasma membranes, retaining their complexity. Therefore, the GPMV isolation procedure described here is a powerful tool that can be used to correlate MPP1 deficiency and plasma membrane organization (26). In our experiments,  $l_o$  and  $l_d$  phase coexistence was observed for all isolated GPMVs (Fig. 5 A), indicating that plasma membranes of all three cell types consist of liquid domains, which coalesce into large  $l_o$ -phases in a temperature-dependent manner. Increased fluidity of nonphase-separated membranes was observed in GPMVs from MPP1-KnD cells measured at RT (Fig. 1, B–D). Moreover, MPP1 reduction destabilized the raft domains, as observed by a significant decrease in  $T_{misc}$  of the  $l_o/l_d$  phases. Of importance, this difference was not caused by major changes in the lipid composition, as the order parameters of liposomes obtained from lipids extracted from GPMVs did not show any differences between control and MPP1-KnD samples (Fig. 3 C). It should be noted that a similar function was recently suggested for palmitoylated Rac1 in COS-7 and MEF cells (41). The proposed mechanism involved an actin cytoskeleton in the raft assembly. In our system this seems not to be the case, as actin is not present in GPMV membranes. Moreover actin detachment from the plasma membrane, via latrunculin or sodium carbonate treatment, had no influence on isolated



DRM profiles (24). Our hypothesis is that, upon palmitoylation, MPP1 is released from the membrane skeleton and is able to act as a membrane-organizing molecule.

Quinn and co-workers have shown that MPP1 is a crucial mediator of chemoattractant-mediated neutrophil membrane polarization, controlled by an unknown mechanism and is accompanied by Akt phosphorylation and the accumulation of PI(3,4,5)P<sub>3</sub> at the leading edge of migrating cells (23). We have previously reported that *MPP1* knock-down in HEL cells leads to changes in signal transduction of the insulin/c-kit cascade, whereas lack of MPP1 palmitoylation in erythrocytes underlie membrane disorder, which causes a significant decrease of DRM presence in these cells and results in hemolytic anemia (24), indicating a crucial physiological role of MPP1 in erythroid membrane organization. To our knowledge, we propose a novel function of the MPP1 protein in organization of the lateral heterogeneity within the membrane. Here, we provide evidence that the presence of MPP1 stabilizes raft domains in cells, as observed by a higher  $T_{\text{misc}}$  of  $l_o/l_d$  phases in GPMVs isolated from control and MPP1-KnD cells.

As they are deprived of intracellular compartments, but maintain the ability to phase separate, plasma membrane vesicles provide an excellent tool for membrane order investigation. Nevertheless, they do suffer from some limitations, such as the loss of native membrane leaflet asymmetry (4). However, from the extensive physicochemical GPMV-membrane analysis presented in this study, we propose that the observed changes in the lateral structure of plasma membrane in erythroid cells are modulated by MPP1. This novel function ascribed to this MAGUK family protein is, to our knowledge, also one of the first cases describing the involvement of a single protein in lateral plasma membrane organization. Our hypothesis, which is now the subject of further research, is that MPP1 binds to preexisting cholesterol/protein nanoassemblies and induces their clustering and stabilization, thereby making them functionally active membrane structures (resting state rafts). Data from our preliminary results indicates that MPP1 binding to the membrane nanoassemblies occurs via interactions with typical raft proteins as flotillins 1 and 2 and probably stomatin. Binding specific lipids cannot also be excluded.

Of importance, although MPP1 expression is restricted mostly to red blood cells, erythroid precursors and other blood cells (Ł. Niemiec, A.B., J.P., M.M., and A.F.S., unpublished data), its homologs, which belong to the MAGUK family, are broadly expressed in various tissues and are well conserved throughout evolution (42,43). The other members of this family are also known to act as scaffolding molecules, maintaining apico-basal polarity and cell junction structure (20,23,43–47). In mammals, PSD-95 and SAP-97 have been identified not only as crucial molecules involved in the maturation of synapses (48,49), but also as molecules important for the clustering and stabilization of

membrane glutamate receptors upon presynaptic and postsynaptic site contact (50). Dlg1 has been found to regulate antigen-induced synaptic-raft and TCR clustering in T cells (51), whereas CARMA, a lymphocyte-specific MAGUK family member, is required for membrane raft localization of transducers engaged in TCR-mediated activation of NF $\kappa$ B (52–54). MAGUKs have been shown to mediate protein-protein interactions in all of these processes. However, it could be envisioned that they also act as allosteric regulators for signal transduction proteins, by influencing the physicochemical properties of the lipid environment for the transmembrane or membrane-associated proteins.

## CONCLUSIONS

The observation of liquid-phases of various compositions and order parameters in plasma membrane-derived vesicles suggests that biological membranes possess complex lateral organization and constitute a mosaic of highly dynamic and transient domains of different compositions and stabilities. Previous reports using this membrane model focused mainly on the physicochemical properties of separated liquid phases, along with factors that could mediate selective partitioning of lipids and proteins to a particular phase (4–6,9,11).

In this report, we have been able to demonstrate that a single protein, MPP1, can directly/or indirectly modulate physicochemical properties of the model, cytoskeleton-depleted membranes of GPMVs by changing their fluidity as well as phase separation behavior. Advanced microscopic methods using order-sensing probes, such as C-laurdan and di-4, showed that, in erythroid cell membrane-derived vesicles, MPP1 plays an important role in maintaining proper order of the membrane (Fig. 1). Moreover, the presence of this protein stabilizes the  $l_o$  phase, as observed in the higher miscibility transition temperature of separated vesicles (Fig. 5). Finally, we showed that changes in membrane fluidity are caused by MPP1, in the absence of major changes in membrane lipid composition, as the fluidity of pure lipids extracted from GPMV membranes remained unchanged (Fig. 3) and MPP1 recovery in KnD cells leads to the reestablishment of plasma membrane organization (Fig. 4).

In summary, we propose that MPP1 acts as an important factor in regulating the fluidity of erythroid plasma membrane-derived vesicles, which reflects domain formation in native membranes. To our knowledge, this is one of the first demonstrations of an individual protein engagement in the changes in physicochemical properties ( $l_o/l_d$  balance) of the plasma membrane of living cell.

## SUPPORTING MATERIAL

Three figures are available at [http://www.biophysj.org/biophysj/supplemental/S0006-3495\(15\)00277-5](http://www.biophysj.org/biophysj/supplemental/S0006-3495(15)00277-5).

## AUTHOR CONTRIBUTIONS

J.P., M.G., and A.F.S. designed research, J.P. performed research, A.B. prepared rescue mutant of MPP1, M.M. performed MPP1 localization experiments, J.P., M.G., and A.F.S. analyzed data and wrote the article.

## ACKNOWLEDGMENTS

We thank Kai Simons for hosting J.P. at his lab and reading the manuscript.

This work was supported by NCN Grant DEC-2012/05/B/NZ1/01638 (J.P., A.B., M.M., and A.F.S.), EMBO Short term fellowship award ASTF 402-2011 (J.P.), the Deutsche Forschungsgemeinschaft “Transregio 83” Grant TRR83 TP18 (M.G.), and by the German Federal Ministry of Education and Research (BMBF) grant to the German Center for Diabetes Research (DZD e.V.) (M.G.). Publication costs were supported by Wrocław Center of Biotechnology, program The Leading National Research Center (KNOW) for years 2014–2018.

## REFERENCES

- Lingwood, D., and K. Simons. 2010. Lipid rafts as a membrane-organizing principle. *Science*. 327:46–50.
- Eggeling, C., C. Ringemann, ..., S. W. Hell. 2009. Direct observation of the nanoscale dynamics of membrane lipids in a living cell. *Nature*. 457:1159–1162.
- Lingwood, D., J. Ries, ..., K. Simons. 2008. Plasma membranes are poised for activation of raft phase coalescence at physiological temperature. *Proc. Natl. Acad. Sci. USA*. 105:10005–10010.
- Baumgart, T., A. T. Hammond, ..., W. W. Webb. 2007. Large-scale fluid/fluid phase separation of proteins and lipids in giant plasma membrane vesicles. *Proc. Natl. Acad. Sci. USA*. 104:3165–3170.
- Levental, I., D. Lingwood, ..., K. Simons. 2010. Palmitoylation regulates raft affinity for the majority of integral raft proteins. *Proc. Natl. Acad. Sci. USA*. 107:22050–22054.
- Levental, I., M. Grzybek, and K. Simons. 2011. Raft domains of variable properties and compositions in plasma membrane vesicles. *Proc. Natl. Acad. Sci. USA*. 108:11411–11416.
- Kaiser, H. J., D. Lingwood, ..., K. Simons. 2009. Order of lipid phases in model and plasma membranes. *Proc. Natl. Acad. Sci. USA*. 106:16645–16650.
- Sezgin, E., I. Levental, ..., P. Schwallie. 2012. Partitioning, diffusion, and ligand binding of raft lipid analogs in model and cellular plasma membranes. *Biochim. Biophys. Acta*. 1818:1777–1784.
- Levental, I., F. J. Byfield, ..., P. A. Janmey. 2009. Cholesterol-dependent phase separation in cell-derived giant plasma-membrane vesicles. *Biochem. J*. 424:163–167.
- Johnson, S. A., B. M. Stinson, ..., T. Baumgart. 2010. Temperature-dependent phase behavior and protein partitioning in giant plasma membrane vesicles. *Biochim. Biophys. Acta*. 1798:1427–1435.
- Zhou, Y., K. N. Maxwell, ..., I. Levental. 2013. Bile acids modulate signaling by functional perturbation of plasma membrane domains. *J. Biol. Chem*. 288:35660–35670.
- Chishti, A. H. 1998. Function of p55 and its nonerythroid homologues. *Curr. Opin. Hematol*. 5:116–121.
- Laura, R. P., S. Ross, ..., L. A. Lasky. 2002. MAGI-1: a widely expressed, alternatively spliced tight junction protein. *Exp. Cell Res*. 275:155–170.
- Sturgill, J. F., P. Steiner, ..., B. L. Sabatini. 2009. Distinct domains within PSD-95 mediate synaptic incorporation, stabilization, and activity-dependent trafficking. *J. Neurosci*. 29:12845–12854.
- Samuels, B. A., Y. P. Hsueh, ..., L. H. Tsai. 2007. Cdk5 promotes synaptogenesis by regulating the subcellular distribution of the MAGUK family member CASK. *Neuron*. 56:823–837.
- Wolburg, H., and A. Lippoldt. 2002. Tight junctions of the blood-brain barrier: development, composition and regulation. *Vascul. Pharmacol*. 38:323–337.
- Beatch, M., L. A. Jesaitis, ..., B. R. Stevenson. 1996. The tight junction protein ZO-2 contains three PDZ (PSD-95/Discs-Large/ZO-1) domains and an alternatively spliced region. *J. Biol. Chem*. 271:25723–25726.
- Haskins, J., L. Gu, ..., B. R. Stevenson. 1998. ZO-3, a novel member of the MAGUK protein family found at the tight junction, interacts with ZO-1 and occludin. *J. Cell Biol*. 141:199–208.
- McAllister-Lucas, L. M., X. Jin, ..., P. C. Lucas. 2010. The CARMA3-Bcl10-MALT1 signalosome promotes angiotensin II-dependent vascular inflammation and atherogenesis. *J. Biol. Chem*. 285:25880–25884.
- Dimitratos, S. D., D. F. Woods, ..., P. J. Bryant. 1999. Signaling pathways are focused at specialized regions of the plasma membrane by scaffolding proteins of the MAGUK family. *BioEssays*. 21:912–921.
- Hata, Y., S. Butz, and T. C. Südhof. 1996. CASK: a novel dlg/PSD95 homolog with an N-terminal calmodulin-dependent protein kinase domain identified by interaction with neuexins. *J. Neurosci*. 16:2488–2494.
- Marfatia, S. M., R. A. Lue, ..., A. H. Chishti. 1994. In vitro binding studies suggest a membrane-associated complex between erythroid p55, protein 4.1, and glycophorin C. *J. Biol. Chem*. 269:8631–8634.
- Quinn, B. J., E. J. Welch, ..., A. H. Chishti. 2009. Erythrocyte scaffolding protein p55/MPP1 functions as an essential regulator of neutrophil polarity. *Proc. Natl. Acad. Sci. USA*. 106:19842–19847.
- Łach, A., M. Grzybek, ..., A. F. Sikorski. 2012. Palmitoylation of MPP1 (membrane-palmitoylated protein 1)/p55 is crucial for lateral membrane organization in erythroid cells. *J. Biol. Chem*. 287:18974–18984.
- Biernatowska, A., J. Podkalicka, ..., A. F. Sikorski. 2013. The role of MPP1/p55 and its palmitoylation in resting state raft organization in HEL cells. *Biochim. Biophys. Acta*. 1833:1876–1884.
- Sezgin, E., H. J. Kaiser, ..., I. Levental. 2012. Elucidating membrane structure and protein behavior using giant plasma membrane vesicles. *Nat. Protoc*. 7:1042–1051.
- Ejsing, C. S., J. L. Sampaio, ..., A. Shevchenko. 2009. Global analysis of the yeast lipidome by quantitative shotgun mass spectrometry. *Proc. Natl. Acad. Sci. USA*. 106:2136–2141.
- Gaus, K., T. Zech, and T. Harder. 2006. Visualizing membrane microdomains by Laurdan 2-photon microscopy. *Mol. Membr. Biol*. 23:41–48.
- Owen, D. M., P. M. Lanigan, ..., A. I. Magee. 2006. Fluorescence lifetime imaging provides enhanced contrast when imaging the phase-sensitive dye di-4-ANEPPDHQ in model membranes and live cells. *Biophys. J*. 90:L80–L82.
- Owen, D. M., S. Oddos, ..., M. Cebecauer. 2010. High plasma membrane lipid order imaged at the immunological synapse periphery in live T cells. *Mol. Membr. Biol*. 27:178–189.
- Lenoir, M., M. Grzybek, ..., M. Overduin. 2015. Structural basis of dynamic membrane recognition by trans-Golgi network specific FAPP proteins. *J. Mol. Biol*. 427:966–981.
- Czogalla, A., M. Grzybek, ..., U. Coskun. 2014. Validity and applicability of membrane model systems for studying interactions of peripheral membrane proteins with lipids. *Biochim. Biophys. Acta*. 1841:1049–1059.
- Hancock, J. F. 2006. Lipid rafts: contentious only from simplistic standpoints. *Nat. Rev. Mol. Cell Biol*. 7:456–462.
- Filipowicz, W., L. Jaskiewicz, ..., R. S. Pillai. 2005. Post-transcriptional gene silencing by siRNAs and miRNAs. *Curr. Opin. Struct. Biol*. 15:331–341.
- Hutvagner, G., M. J. Simard, ..., P. D. Zamore. 2004. Sequence-specific inhibition of small RNA function. *PLoS Biol*. 2:E98.

36. Simons, K., and M. J. Gerl. 2010. Revitalizing membrane rafts: new tools and insights. *Nat. Rev. Mol. Cell Biol.* 11:688–699.
37. Sengupta, P., A. Hammond, ..., B. Baird. 2008. Structural determinants for partitioning of lipids and proteins between coexisting fluid phases in giant plasma membrane vesicles. *Biochim. Biophys. Acta.* 1778:20–32.
38. Ayuyan, A. G., and F. S. Cohen. 2008. Raft composition at physiological temperature and pH in the absence of detergents. *Biophys. J.* 94:2654–2666.
39. Veatch, S. L., P. Cicuta, ..., B. Baird. 2008. Critical fluctuations in plasma membrane vesicles. *ACS Chem. Biol.* 3:287–293.
40. van Meer, G., D. R. Voelker, and G. W. Feigenson. 2008. Membrane lipids: where they are and how they behave. *Nat. Rev. Mol. Cell Biol.* 9:112–124.
41. Navarro-Lérida, I., S. Sánchez-Perales, ..., M. A. Del Pozo. 2012. A palmitoylation switch mechanism regulates Rac1 function and membrane organization. *EMBO J.* 31:534–551.
42. te Velthuis, A. J., J. F. Admiraal, and C. P. Bagowski. 2007. Molecular evolution of the MAGUK family in metazoan genomes. *BMC Evol. Biol.* 7:129.
43. Oliva, C., P. Escobedo, ..., J. Sierralta. 2012. Role of the MAGUK protein family in synapse formation and function. *Dev. Neurobiol.* 72:57–72.
44. Funke, L., S. Dakoji, and D. S. Bredt. 2005. Membrane-associated guanylate kinases regulate adhesion and plasticity at cell junctions. *Annu. Rev. Biochem.* 74:219–245.
45. Caruana, G. 2002. Genetic studies define MAGUK proteins as regulators of epithelial cell polarity. *Int. J. Dev. Biol.* 46:511–518.
46. Woods, D. F., and P. J. Bryant. 1991. The discs-large tumor suppressor gene of *Drosophila* encodes a guanylate kinase homolog localized at septate junctions. *Cell.* 66:451–464.
47. Woods, D. F., C. Hough, ..., P. J. Bryant. 1996. Dlg protein is required for junction structure, cell polarity, and proliferation control in *Drosophila* epithelia. *J. Cell Biol.* 134:1469–1482.
48. Nikonenko, I., B. Boda, ..., D. Muller. 2008. PSD-95 promotes synaptogenesis and multiinnervated spine formation through nitric oxide signaling. *J. Cell Biol.* 183:1115–1127.
49. Poglia, L., D. Muller, and I. Nikonenko. 2011. Ultrastructural modifications of spine and synapse morphology by SAP97. *Hippocampus.* 21:990–998.
50. Waites, C. L., A. M. Craig, and C. C. Garner. 2005. Mechanisms of vertebrate synaptogenesis. *Annu. Rev. Neurosci.* 28:251–274.
51. Round, J. L., T. Tomassian, ..., M. C. Miceli. 2005. Dlg1 coordinates actin polymerization, synaptic T cell receptor and lipid raft aggregation, and effector function in T cells. *J. Exp. Med.* 201:419–430.
52. Hara, H., T. Wada, ..., J. M. Penninger. 2003. The MAGUK family protein CARD11 is essential for lymphocyte activation. *Immunity.* 18:763–775.
53. Jun, J. E., L. E. Wilson, ..., C. C. Goodnow. 2003. Identifying the MAGUK protein Carma-1 as a central regulator of humoral immune responses and atopy by genome-wide mouse mutagenesis. *Immunity.* 18:751–762.
54. Wang, D., R. Matsumoto, ..., X. Lin. 2004. CD3/CD28 costimulation-induced NF-kappaB activation is mediated by recruitment of protein kinase C-theta, Bcl10, and IkappaB kinase beta to the immunological synapse through CARMA1. *Mol. Cell. Biol.* 24:164–171.

## Membrane Palmitoylated Protein 1 (MPP1) acts as a tuning factor regulating phase separation abilities of Giant Plasma Membrane-derived Vesicles.

Joanna Podkalicka<sup>1,4</sup>, Agnieszka Biernatowska<sup>1</sup>, Michał Majkowski<sup>1</sup>, Michał Grzybek<sup>2,3</sup> and Aleksander F. Sikorski<sup>1\*</sup>

<sup>1</sup> Laboratory of Cytobiochemistry, Faculty of Biotechnology, University of Wrocław, F. Joliot-Curie 14a, 50-383 Wrocław, Poland,

<sup>2</sup> Paul Langerhans Institute Dresden of the Helmholtz Centre Munich at the University Clinic Carl Gustav Carus, TU Dresden, Fetscher Str. 74, 01307 Dresden, Germany

<sup>3</sup> German Center for Diabetes Research (DZD), Ingolstädter Landstraße 1, 85764 Neuherberg, Germany

<sup>4</sup> Max Planck Institute of Molecular Cell Biology and Genetics, Pfotenhauerstr. 108, 01307 Dresden, Germany

### Supporting material

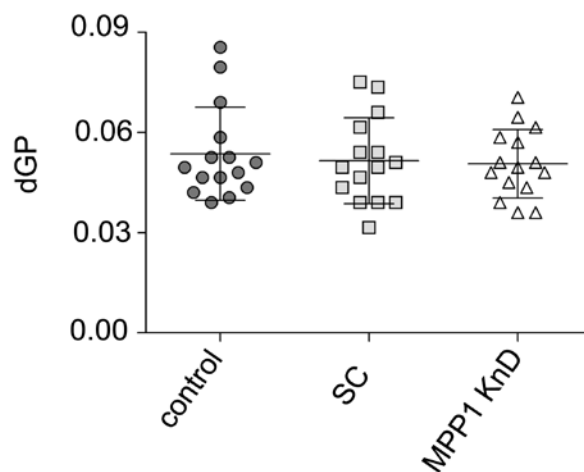


**Fig. S1.  $\Delta GP$  is constant for all isolated GPMVs.** Quantitative analysis of  $\Delta GP$  distribution in GPMVs obtained from MPP1-KnD and control cells shows no significant difference in the absence of MPP1. Each point is representative of >40 vesicles per cell-type.

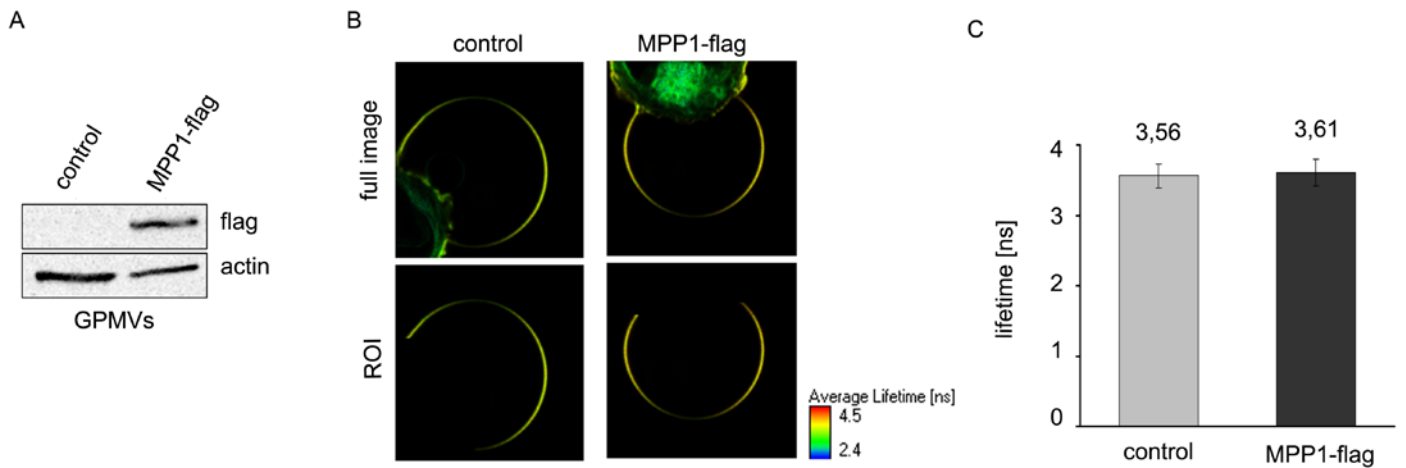


**Fig. S2. MPP1 overexpression does not increase membrane order of GPMVs isolated from HEL cells. (A)** Western Blot analysis of MPP1-flag expression level in GPMVs derived from HEL cells. **(B)** Representative FLIM images of di-4 stained GPMVs isolated from control and MPP1-flag transfected cells (the longer the fluorescence lifetime values, the more ordered the membrane; all images taken at 23°C). **(C)** Mean fluorescence-lifetime values averaged of >15 vesicles per cell type. ROI – region of interest.

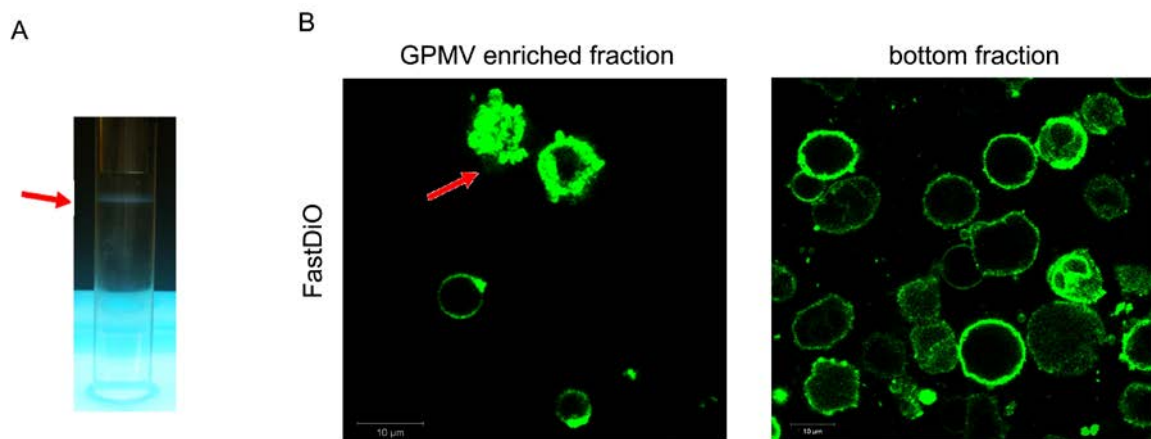


**Fig. S3. GPMV enriched fraction contains also other membranes. (A)** GPMV enriched fraction after gradient separation. **(B)** Representative images of Fast-DiO stained membranes. Within GPMV-enriched fraction cell debris are detected. Bottom fraction contains predominantly cells but some of retaining GPMVs are also observed.